Geophys. J. Int. (2008) **173,** 693–702 doi: 10.1111/j.1365-246X.2008.03745.x

Viscous heating, adiabatic heating and energetic consistency in compressible mantle convection

Wei Leng and Shijie Zhong

Department of Physics, University of Colorado at Boulder, Boulder, CO 80309*, USA. E-mail: wei.leng@colorado.edu*

Accepted 2008 January 23. Received 2008 January 22; in original form 2007 October 2

SUMMARY

Although it has been suggested that the total viscous heating, Q_v, should be exactly balanced by the total adiabatic heating, Q_a, for compressible mantle convection, previous numerical studies show a significant imbalance of up to several percent between Q_v and Q_a for simple isoviscous compressible convection. The cause of this imbalance and its potential effects on more complicated convective systems remain largely unknown. In this study, we present an analysis to show that total viscous heating and adiabatic heating for compressible mantle convection with anelastic liquid approximation (ALA) and the Adams–Williamson equation of state are balanced out at any instant in time, and that the previously reported imbalance between Q_v and Q_a for numerical models with a truncated anelastic liquid approximation (TALA) is caused by neglecting the effect of the pressure on the buoyancy force. Although we only consider the Adams–Williamson equation of state in our analysis, our method can be used to check the energetic consistency for other forms of equation of state. We formulate numerical models of compressible mantle convection under both TALA and ALA formulations by modifying the Uzawa algorithm in Citcom code. Our numerical results confirm our analysis on the balance between total viscous heating and total adiabatic heating.

Key words: Numerical solutions; Mantle processes; Equations of state.

1 INTRODUCTION

Although most mantle convection studies assume an incompressible mantle with Boussinesq (Spiegel & Veronis 1960; Mihaljan 1962) or extended-Boussinesq approximation (Christensen & Yuen 1985; Zhong 2006), mantle compressibility may be needed to better integrate seismology and mineral physics into dynamic models of the mantle. Mantle compressibility affects not only the average temperature distribution of the mantle, but also the flow pattern and convective vigour (Jarvis & McKenzie 1980). Jarvis & McKenzie (1980) formulated the first compressible mantle convection models with an anelastic liquid approximation (ALA). However, most of the studies, including Jarvis & McKenzie (1980), only use a truncated anelastic liquid approximation (TALA) in which the effect of the pressure on the buoyancy force is ignored (e.g. Ita & King 1994; Tan & Gurnis 2005).

Viscous heating due to the dissipation and adiabatic heating due to the work done by the fluid in adiabatic volume change are two important energy terms in compressible mantle convection (Bercovici *et al.* 1992; Balachandar *et al.* 1995). Although it has been demonstrated that the total viscous heating, Q_v, should be exactly balanced by the total adiabatic heating, Q_a (Turcotte *et al.* 1974; Hewitt *et al.* 1975; Zhang & Yuen 1996a, b), numerical results from simple TALA models with uniform material and thermodynamic properties showed that there can be some significant, up to several percent, imbalance between Q_v and Q_a (Jarvis & McKenzie 1980), indicating an energetic inconsistency with these models. The cause for the imbalance and energetic inconsistency is not well understood. Furthermore, it is unclear how the imbalance is affected by realistic and variable material properties and thermodynamic properties or different equation of state.

In this study, we investigate the cause for the imbalance between viscous heating and adiabatic heating in TALA models, and examine the conditions for energetic consistency in compressible mantle convection. In the following sections, we will first present the governing equations for compressible mantle convection with an ALA. We then analytically demonstrate on the basis of the momentum equation that the total adiabatic heating and viscous heating must be exactly balanced for ALA formulation at any time for a convective system and that the imbalance between them for TALA is caused by the neglected pressure term in the buoyancy. Then, we present an algorithm for numerically modelling compressible mantle convection and show that our numerical models are consistent with our analysis. The main conclusions are presented at the end.

2 FORMULATION OF COMPRESSIBLE MANTLE CONVECTION

For thermal convection in a compressible fluid with an ALA and an infinite Prandtl number, the equations of conservation of the mass, momentum and energy can be written as following (Jarvis & McKenzie 1980):

$$(\rho_r u_i)_{,i} = 0, \tag{1}$$

$$-p_{,j}\delta_{ij} + \tau_{ij,j} - \Delta\rho g \delta_{i3} = 0, \tag{2}$$

$$\rho_r C_p \dot{T} + \rho_r C_p u_i T_{,i} + \rho_r g \alpha T u_3 = (kT_{,i})_{,i} + \tau_{ij} u_{i,j} + \rho_r H, \tag{3}$$

where ρ_r, u, p, τ, $\Delta\rho$, g, C_p, T, α, k and H are radial density, velocity vector, dynamic pressure, deviatoric stress tensor, density anomalies, gravitational acceleration, specific heat at constant pressure, temperature, coefficient of thermal expansion, thermal conductivity and heat production rate, respectively; i and j are spatial indices and three means vertical direction; δ is the Kronecker delta function. $\dot{T}$ is the derivative of temperature with respect to time t. The gravitational acceleration g and thermodynamic parameters including C_p, α and k are assumed to be depth-dependent in the mantle.

The radial density distribution in the Earth's mantle is determined by the equation of state. We use the Adams–Williamson equation of state by Birch (1952) to describe the adiabatic density distribution in the mantle:

$$\frac{1}{\rho_r}\frac{\mathrm{d}\rho_r}{\mathrm{d}z} = -\frac{\alpha g}{C_p \Gamma}, \tag{4}$$

where z is the vertical (i.e. radial) coordinate (the z-axis pointing upward); Γ is the depth-dependent Grüneisen's parameter and is defined as

$$\Gamma = \frac{\alpha K_s}{\rho_r C_p}, \tag{5}$$

where K_s is the adiabatic bulk modulus. The Adams–Williamson equation is simple, but provides a good approximation for the adiabatic density distribution in the mantle. However, it should be pointed out that although many studies use the Adams–Williamson equation, other forms of equation of state may also be used for the compressible mantle convection.

Suppose that density $\rho = \rho\,(T, P)$, where P is the hydrostatic pressure, the density perturbation is given as (Jarvis & McKenzie 1980):

$$\Delta\rho = \rho_r\big[-\alpha(T - T_r) + K_T^{-1} p\big], \tag{6}$$

where T_r is a radial reference temperature and K_T is the isothermal bulk modulus. Here we assume that in our models K_s is approximately equal to K_T. It should be pointed out that this assumption ignores the thermodynamic constraints on K_s and K_T and simplifies the compressible mantle convection problem as discussed in Schubert *et al.* (2001).

Eqs (1)–(4) can be non-dimensionalized with the following characteristic values:

$$\begin{aligned} &x_i = \mathrm{d}x_i', \quad u_i = \frac{\kappa_0}{d}u_i', \quad T = \Delta T T' + T_s, \quad T_s = \Delta T T_s', \quad \rho_r = \rho_0 \rho_r', \\ &t = \frac{d^2}{\kappa_0}t', \quad H = \frac{H'\kappa_0 \Delta T C_{p\_0}}{d^2}, \quad \eta = \eta_0 \eta', \quad p = \frac{\eta_0 \kappa_0}{d^2}p', \quad \alpha = \alpha_0 \alpha', \\ &g = g_0 g', \quad C_p = C_{p\_0} C_p', \quad \Gamma = \Gamma_0 \Gamma', \quad k = k_0 k', \end{aligned} \tag{7}$$

where symbols with primes are dimensionless; d, κ_0, ΔT, T_s, ρ_0, t, η, η_0, α_0, g_0, C_{p_0}, Γ_0 and k_0 are mantle thickness, reference thermal diffusivity, temperature contrast across the layer, surface temperature, reference density, time, viscosity, reference viscosity, reference coefficient of thermal expansion, reference gravitational acceleration, reference specific heat at constant pressure, reference Grüneisen's parameter and reference thermal conductivity, respectively. The reference thermal diffusivity is defined as $\kappa_0 = k_0/(\rho_0 C_{p\_0})$.

The details for non-dimensionalizing the governing equations can be found in Schubert *et al.* (2001). After dropping the primes, the dimensionless governing equations for ALA are as following:

$$(\rho_r u_i)_{,i} = 0, \tag{8}$$

$$-p_{,j}\delta_{ij} + \tau_{ij,j} + \left[\rho_r \alpha g Ra (T - T_r) - \frac{\alpha g}{C_p \Gamma} p\gamma\right]\delta_{i3} = 0, \tag{9}$$

$$\rho_r C_p \dot{T} + \rho_r C_p u_i T_{,i} + \rho_r \alpha g D_i u_3 (T + T_s) = (kT_{,i})_{,i} + \frac{D_i}{Ra}\tau_{ij} u_{i,j} + \rho_r H, \tag{10}$$

where $D_i = \alpha_0 g_0 d/C_{p\_0}$ is the dissipation number; $Ra = \rho_0 \alpha_0 g_0 \Delta T d^3/(\kappa_0 \eta_0)$ is the Rayleigh number; $\gamma = D_i/\Gamma_0$ is defined as the mantle compressibility.

The dimensionless Adams–Williamson equation is

$$\frac{1}{\rho_r}\frac{\mathrm{d}\rho_r}{\mathrm{d}z} = -\frac{\alpha g}{C_p \Gamma}\gamma. \tag{11}$$

It should be noted that the effect of dynamic pressure on the buoyancy force is included in the momentum eq. (9). Ignoring this term leads to a formulation with TALA, and the momentum equation becomes (Jarvis & McKenzie 1980; Ita & King 1994; Tan & Gurnis 2005)

$$-p_{,j}\delta_{ij} + \tau_{ij,j} + \rho_r \alpha g Ra (T - T_r)\delta_{i3} = 0. \tag{12}$$

3 VISCOUS HEATING AND ADIABATIC HEATING IN COMPRESSIBLE MANTLE CONVECTION

It has been shown that the total viscous heating and adiabatic heating are exactly balanced out for steady-state convection based on energy balance argument from the energy equation (Turcotte *et al.* 1974; Hewitt *et al.* 1975). Zhang & Yuen (1996a) indicated that the total viscous heating and adiabatic heating should be balanced out at any instant of time based on the momentum equation. However, none of these studies provides an explanation to the imbalance between these two energy terms in previous models of compressible mantle convection. Here, following the suggestion in considering viscous heating and adiabatic heating from the momentum equation by Zhang & Yuen (1996a), we examine in details the conditions for energetic consistency for compressible mantle convection, that is, the conditions under which the total viscous heating and adiabatic heating are exactly balanced out.

For the momentum eq. (9), we may multiply velocity u_i to both sides and integrate for the whole volume,

$$-\int p_{,i}u_i \mathrm{d}V + \int \tau_{ij,j}u_i \mathrm{d}V + \int \left[\rho_r \alpha g Ra(T - T_r) - \frac{\alpha g}{C_p \Gamma} p\gamma\right] u_3 \mathrm{d}V = 0. \tag{13}$$

Note that

$$\int \tau_{ij,j}u_i \mathrm{d}V = \oint \tau_{ij}u_i \mathrm{d}S_j - \int \tau_{ij}u_{i,j} \mathrm{d}V, \tag{14}$$

where the surface integral is for the entire surface bounded the domain and S_j is the outward unit vector normal to the surface. In a closed system where there is no material exchange between the system and outside, for both free-slip boundary conditions and no-slip boundary conditions, we have

$$\oint \tau_{ij}u_i \mathrm{d}S_j = 0 \tag{15}$$

and

$$\int \tau_{ij,j}u_i \mathrm{d}V = -\int \tau_{ij}u_{i,j} \mathrm{d}V. \tag{16}$$

A similar reasoning leads to

$$\int p_{,i}u_i \mathrm{d}V = -\int p u_{i,i} \mathrm{d}V. \tag{17}$$

Therefore, eq. (13) becomes

$$\int p u_{i,i} \mathrm{d}V - \int \tau_{ij}u_{i,j} \mathrm{d}V + \int \left[\rho_r \alpha g Ra(T - T_r) - \frac{\alpha g}{C_p \Gamma} p\gamma\right] u_3 \mathrm{d}V = 0. \tag{18}$$

From the mass conservation eq. (8) and the Adams–Williamson eq. (11),

$$u_{i,i} = -\frac{(\rho_r)_{,i}}{\rho_r}u_i = -\frac{1}{\rho_r}\frac{\mathrm{d}\rho_r}{\mathrm{d}z}u_3 = \frac{\alpha g}{C_p \Gamma}u_3 \gamma. \tag{19}$$

Substituting eq. (19) into eq. (18) leads to

$$\int \frac{\alpha g}{C_p \Gamma} p u_3 \gamma \mathrm{d}V - \int \tau_{ij}u_{i,j} \mathrm{d}V + \int \left[\rho_r \alpha g Ra(T - T_r) - \frac{\alpha g}{C_p \Gamma} p\gamma\right] u_3 \mathrm{d}V = 0. \tag{20}$$

Note that in eq. (20) the first integral associated with dynamic pressure p cancels exactly the pressure term in the third integral. Multiplying dissipation number D_i to both sides of eq. (20) and re-arranging it lead to

$$\frac{D_i}{Ra}\int \tau_{ij}u_{i,j} \mathrm{d}V = D_i \int \rho_r \alpha g(T - T_r)u_3 \mathrm{d}V. \tag{21}$$

On any horizontal plane A that slices through the entire domain, due to the mass conservation,

$$\int \rho_r \alpha g u_3 \mathrm{d}A = 0. \tag{22}$$

Consequently, for any depth-dependent reference temperature T_r or constant surface temperature T_s, we have

$$\int \rho_r \alpha g u_3 T_r \mathrm{d}V = \int \rho_r \alpha g u_3 T_s \mathrm{d}V = 0. \tag{23}$$

Upon substituting eqs (23) into (21), we obtain

$$\frac{D_i}{Ra}\int \tau_{ij}u_{i,j} \mathrm{d}V = D_i \int \rho_r \alpha g(T + T_s)u_3 \mathrm{d}V. \tag{24}$$

In eq. (24), $Q_v = \frac{D_i}{Ra}\int \tau_{ij}u_{i,j} \mathrm{d}V$, is the total viscous heating (i.e. the volumetric integral of the second term on the right-hand side of the energy eq. 10), and $Q_a = D_i \int \rho_r \alpha g(T + T_s)u_3 \mathrm{d}V$ is the total adiabatic heating (i.e. the volumetric integral of the third term on the left-hand side of the energy eq. 10). Therefore, combining conservation equations of the mass and momentum, this analysis demonstrates that the total viscous heating and adiabatic heating exactly cancel each other. The fact that our analysis only involves the conservation equations of the mass and momentum indicates that the total viscous heating and adiabatic heating should balance each other at any time for steady state and time-dependent convection in ALA formulation. However, if the pressure effect on the buoyancy force is ignored as done in TALA, it is clear

from our analysis that the two pressure terms in eq. (20) will not cancel each other, and neither do Q_v and Q_a cancel each other. This explains why in TALA models (e.g. Jarvis & McKenzie 1980) the total viscous heating and adiabatic heating are not balanced.

This analysis has two implications for the issue of energetic consistency in compressible mantle convection. First, our analysis demonstrates that the Adams–Williamson equation of state is energetically consistent for compressible mantle convection with depth-dependent thermodynamic parameters and material properties. It should be pointed out that our analysis does not have any restriction to viscosity and is, therefore, applicable to variable viscosity structure. Second, our analysis provides a way to analyze energetic consistency in mantle convection. We think that energetic consistency is an important issue in mantle convection that should be carefully analysed when new formulations of mantle convection or equation of state (e.g. Connolly, 2005) are employed.

4 NUMERICAL EXPERIMENTS FOR TALA AND ALA MODELS

To demonstrate that the imbalance between total viscous heating and adiabatic heating seen in previous numerical models of TALA (Jarvis & McKenzie 1980) is indeed caused by ignoring the pressure in the buoyancy term, we have formulated numerical models of compressible mantle convection for both ALA and TALA approximations.

The numerical models are implemented by solving the governing eqs (8)–(10) with a finite element method. We modify the 2-D Cartesian numerical code Citcom (Moresi & Solomatov 1995) to incorporate the compressibility as well as adiabatic heating and viscous heating terms. Citcom was originally developed to solve the thermal convection problems for incompressible media with the Boussinesq approximation. While it is relatively straightforward to modify the energy equation solver to include the additional heating terms, significantly more effort is needed to deal with the compressibility.

For simplification, we assume that the gravitational acceleration g, mantle viscosity and thermodynamic variables (e.g. α, C_p, Γ and k) are constant in our numerical models. Therefore, in eqs (8)–(12), dimensionless g, α, C_p, Γ and k all become to be one. Eq. (11) can be integrated to obtain the adiabatic density distribution

$$\rho_r(z) = \rho_0 \exp[(1 - z)\gamma]. \tag{25}$$

Note that if the gravitational acceleration and thermodynamic variables in eq. (11) are considered as depth-dependent, the density distribution needs to be obtained from properly integrating eq. (11) in order to maintain energetic consistency.

We first discuss solutions of the Stokes flow problem with compressibility (i.e. eqs (8) and (9)). Citcom uses an Uzawa algorithm to solve the Stokes flow problem. We modified the Uzawa algorithm to take into account of compressibility (see Appendix A). The numerical solutions for the Stokes flow problem can be checked against the analytic solutions based on a propagator matrix method (Hager & O'Connell 1979; Zhong & Zuber 2000) (see Appendix B).

We start from an isoviscous case TALA1 with truncated ALA and $\gamma = 0.25$, which corresponds to a factor of 1.28 density increase from the surface to the bottom boundaries. The boundary conditions for this case are free-slip boundary conditions for top and bottom boundaries and reflecting boundary conditions for vertical sidewalls. The buoyancy force comes from temperature perturbation which is given as:

$$T(x, z) = \delta(z - 0.5)\cos(\pi x). \tag{26}$$

Using the propagator matrix method in Appendix B, analytic solutions for the horizontal velocity and vertical normal stress at the surface are obtained and shown in Table 1. For the same case, we solve the Stokes flow problem using our modified Citcom in a 1×1 box with resolution 128×128 uniform elements. The results are also shown in Table 1. From Table 1, it can be observed that for case TALA1, the analytic and numerical solutions for the Stokes flow problem agree very well.

After adding the pressure term to the buoyancy force, we compute case ALA1 with $\gamma = 0.25$. The difference between analytic and numerical solutions is also negligible (Table 1). A comparison between TALA1 and ALA1 shows, however, that the difference between results from TALA and that from ALA is rather notable, 1.8 and 3.8% for surface velocity and stress, respectively.

We increase the compressibility to $\gamma = 0.5$ and 1.0, which correspond to a factor of 1.65 and 2.72 density contrast across the layer, and compute cases TALA2, TALA3, ALA2 and ALA3 (Table 1). Similarly, we observe that the analytic and numerical solutions agree with each other very well. The difference between TALA and ALA models, however, increases with compressibility. For cases TALA3 and ALA3, the differences are 10.5 and 19.4% for surface velocity and stress, respectively (Table 1).

Table 1. Benchmarks for the 2-D Cartesian compressible Stoke flow problem[a].

Cases	γ	V_s(ana)	V_s	ε_V(%)	S_{rr}(ana)	S_{rr}	ε_S(%)
TALA1	0.25	0.054235	0.054238	0.01	0.56656	0.56651	0.01
TALA2	0.50	0.064294	0.064299	0.01	0.65984	0.65976	0.01
TALA3	1.00	0.090006	0.090012	0.01	0.89406	0.89394	0.01
ALA1	0.25	0.053271	0.053265	0.01	0.54588	0.54569	0.03
ALA2	0.50	0.061732	0.061686	0.07	0.60956	0.60888	0.11
ALA3	1.00	0.081418	0.081159	0.32	0.74864	0.74562	0.40

[a] γ, V_s and S_{rr} are compressibility, horizontal velocity at the surface and radial stress at the surface, respectively. Values with '(ana)' represent the results from analytic solutions. ε_V(%) and ε_S(%) represent the relative errors between analytic solutions and numerical solutions for V_s and S_{rr}, respectively.

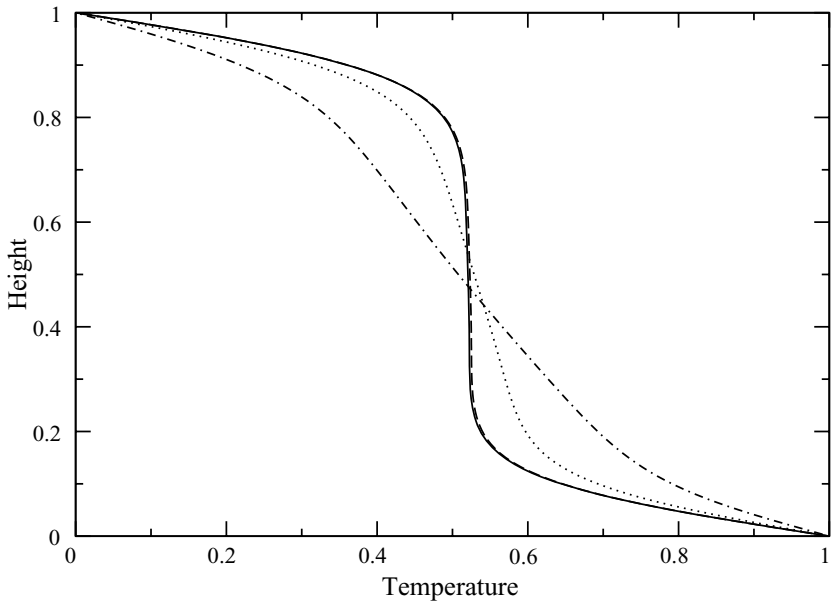

Figure 1. The distribution of horizontally averaged temperature versus vertical height. The solid, dashed, dotted and dash–dotted lines are for cases TALA_C1, ALA_C1, TALA_C2 and TALA_C3, respectively.

Table 2. Numerical results for TALA and ALA convection cases[a].

Cases	Ra	γ	$q_{\rm ave}$	$V_{\rm ave}$	Q_v	Q_a	$\varepsilon_E(\%)$
TALA_C1	10^4	0.25	4.43	39.3	0.8547	0.8523	0.28
TALA_C2	10^4	0.50	3.86	36.1	1.4078	1.3914	1.16
TALA_C3	10^4	1.00	2.57	26.4	1.4614	1.3974	4.38
TALA_C4	10^5	0.50	7.63	165.0	3.2763	3.2484	0.85
TALA_C5	10^5	1.00	3.92	91.2	2.8190	2.7559	2.24
TALA_C6	10^5	2.00	1.58	22.8	0.5702	0.5522	3.16
ALA_C1	10^4	0.25	4.41	38.9	0.8500	0.8504	0.05
ALA_C2	10^4	0.50	3.82	35.0	1.3778	1.3792	0.10
ALA_C3	10^4	1.00	2.47	24.3	1.3542	1.3587	0.34
ALA_C4	10^5	0.50	7.56	161.5	3.2287	3.2322	0.11
ALA_C5	10^5	1.00	3.88	88.9	2.7566	2.7635	0.25
ALA_C6	10^5	2.00	1.41	20.1	0.4727	0.4752	0.53

[a] Ra, γ, q_{ave}, V_{ave}, Q_v and Q_a are the Rayleigh number, compressibility, horizontally averaged surface heat flux, horizontally averaged surface velocity, total viscous heating, and total adiabatic heating, respectively. $\varepsilon_E(\%)$ represents the relative difference between Q_a and Q_v. The cases are all isoviscous and all the results are computed after the system reaches to steady state.

After having validated our solver for the Stokes flow problem with compressibility, to examine the validity of our analysis for viscous heating and adiabatic heating, we compute compressible thermal convection cases in which the energy eq. (10) is also solved. The energy equation is solved by streamline upwind Petrov–Galerkin method (Brooks & Hughes 1982). In the energy equation, the dimensional surface temperature and temperature contrast across the layer are 273 and 3000 K, respectively. The heat production rate H is set to be zero. The top and bottom boundaries are isothermal with dimensionless temperature 0.0 at the top boundary and 1.0 at the bottom boundary. The reference Grüneisen's parameter Γ_0 is set to be 1. Since $\gamma = D_i/\Gamma_0$, the dissipation number D_i is identical to γ. The numerical resolution is 128×128 elements in a 1×1 box with grid refinements near top and bottom boundaries.

We first present results for case TALA_C1 which uses a TALA, $Ra = 10^4$ and $\gamma = 0.25$. We use our modified Citcom and compute this case till it reaches a steady state. Outside of the top and bottom thermal boundary layers, the horizontally averaged temperature increases adiabatically with depth due to the compressibility (Fig. 1). The dimensionless horizontally averaged surface heat flux $q_{\rm ave}$ and surface velocity $V_{\rm ave}$ are 4.43 and 39.3, respectively (Table 2). For this case, the relative difference between total adiabatic heating Q_a and total viscous heating Q_v, ε_E, is 0.28% (Table 2). We then compute case ALA_C1 which uses ALA and is identical to case TALA_C1 except that the pressure effect on the buoyancy force is included. The horizontally averaged temperature is slightly higher for case ALA_C1 than that for case TALA_C1 (Fig. 1). Now, the relative difference between Q_a and Q_v, ε_E, is reduced to 0.05% for case ALA_C1. Note that ε_E for both TALA_C1 and ALA_C1 are negligibly small.

For cases TALA_C2 and TALA_C3, γ is increased to 0.50 and 1.0, respectively, while other parameters remain the same as in case TALA_C1. The increased γ leads to increased adiabatic temperature gradient (Fig. 1). For these two TALA cases, ε_E increases and is as large

as 4.38% for case TALA_C3 (Table 2), which is similar to that found by Jarvis & McKenzie (1980). However, for the two corresponding ALA cases ALA_C2 and ALA_C3, ε_E are 0.10 and 0.34%, respectively (Table 2), which are about one order magnitude smaller than those for TALA cases.

We computed additionally three sets of TALA and ALA models with $\gamma = 0.50$, 1.00 and 2.00, but Rayleigh number of 10^5 (case TALA_C4, TALA_C5, TALA_C6 and ALA_C4, ALA_C5, ALA_C6 in Table 2). The results show similar features: for TALA cases, the relative difference between Q_a and Q_v, ε_E increases with γ and can be as large as 3.16%; but for ALA cases, ε_E are about one order magnitude smaller (Table 2). Note that due to numerical errors that exist for any numerical solutions, slight imbalance between Q_a and Q_v is expected even for ALA cases. These results are in a complete agreement with our analysis presented in the last section that for steady state convection, the imbalance between total viscous heating and total adiabatic heating seen in previous TALA models is caused by neglecting the pressure effect on the buoyancy term. Note that for cases TALA_C6 and ALA_C6, we increase the resolution from 128 × 128 elements to 256 × 256 elements to better resolve the large density variation from the surface to the bottom.

It is also interesting to examine how the total viscous heating and adiabatic heating are balanced for non-steady state or time-dependent convection. We take the steady state temperature field from case TALA_C3, arbitrarily increase the dimensionless temperature by 0.2 everywhere but limiting temperature no greater than 1.0, and compute this model till it returns to a steady state. We then decrease the dimensionless temperature everywhere by 0.2 but limiting temperature no less than 0.0, and again compute it to a steady state. The bulk average temperature and total viscous heating versus time for this experiment are shown in Figs 2a and b. Significant imbalance between Q_a and Q_v exists not

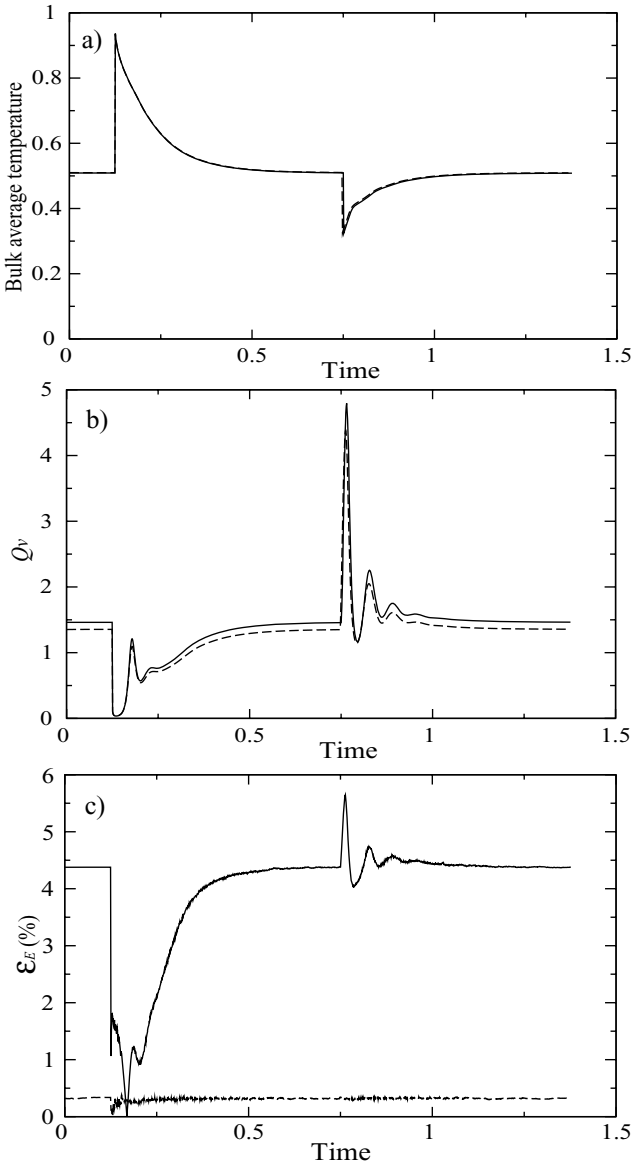

Figure 2. The time-dependence of bulk average temperature (a), the total viscous heating Q_v (b), and the relative difference between total viscous heating and total adiabatic heating ε_E (c), for the transient modelling of cases TALA_C3 (solid line) and ALA_C3 (dashed line).

only for steady state convection, but also for transient convection (Fig. 2c for ε_E). We repeated this sequence of modelling for the ALA model case ALA_C3, and the relative difference between Q_a and Q_v, ε_E, is one order of magnitude smaller compared with TALA_C3 (Fig. 2c), completely agreeing with our analysis.

5 CONCLUSIONS

In this study, we present an analysis to demonstrate that compressible mantle convection with an ALA, the Adams–Williamson equation of state, and depth-dependent thermodynamic parameters, is energetically consistent with total viscous heating and total adiabatic heating that are exactly balanced at any instant in time. Our analysis also shows that the previously reported imbalance between total viscous heating and adiabatic heating for compressible mantle convection with a TALA results from neglecting the effect of the pressure on the buoyancy force. Our analysis is derived from considerations of the conservation equations of the mass and momentum with no involvement of the energy equation, although viscous heating and adiabatic heating terms are directly related to the energy equation. To better study the energy balance for compressible mantle convection, ALA formulation is preferred over TALA, especially for planetary mantles with large compressibility (e.g. within giant planets). Furthermore, the analysis presented in this study provides a method to check whether a given equation of state or a formulation of mantle convection is energetically consistent in compressible mantle convection.

We formulate numerical models of compressible mantle convection under both TALA and ALA formulations by modifying the Uzawa algorithm in Citcom code. By comparing with analytic solutions for the compressible Stokes flow problem, our benchmark studies validate our numerical solutions. Our numerical models of compressible mantle convection for both TALA and ALA confirm our analysis on the balance between total viscous heating and total adiabatic heating. Our modified Uzawa algorithm for compressible mantle convection is sufficiently general and is already extended to 3-D Cartesian and spherical models in codes CitcomCU and CitcomS.

ACKNOWLEDGMENT

The authors thank Eh Tan and an anonymous reviewer for constructive reviews that significantly improve the manuscript. This study is supported by National Science Foundation and David and Lucile Packard Foundation.

REFERENCES

Balachandar, S., Yuen, D.A., Reuteler, D.M. & Lauer, G.S., 1995. Viscous dissipation in three-dimensional convection with temperature-dependent viscosity, *Science,* **267,** 1150–1153.

Bercovici, D., Schubert, G. & Glatzmaier, G.A., 1992. Three-dimensional convection of an infinite-Prandtl number compressible fluid in a basally heated spherical shell, *J. Fluid Mech.,* **239,** 683–719.

Birch, F., 1952. Elasticity and constitution of the Earth's interior, *J. Geophys. Res.,* **57,** 227–286.

Brooks, A.N. & Hughes, T.J.R., 1982. Streamline upwind/Petrov-Galerkin formulations for convection dominated flows with particular emphasis on the incompressible Navier-Stokes equations, *Comp. Meth. Appl. Mech. Eng.,* **32,** 199.

Christensen, U.R. & Yuen, D.A., 1985. Layered convection induced by phase transitions, *J. geophys. Res.,* **90,** 10 291–10 300.

Connolly, J.A.D., 2005. Computation of phase equilibria by linear programming: a tool for geodynamic modeling and its application to subduction zone decarbonation, *Earth planet. Sci. Lett.,* **236,** 524–541.

Hager, B.H. & O'Connell, R.J., 1979. Kinematic models of large-scale flow in the Earth's mantle, *J. geophys. Res.,* **84,** 1031–1048.

Hewitt, J.M., McKenzie, D.P. & Weiss, N.O., 1975. Dissipative heating in convective flows, *J. Fluid Mech.,* **68,** 721–738.

Hughes, T.J.R., 2000. *The Finite Element Method: Linear Static and Dynamic Finite Element Analysis,* 683 pp., Dover Pub., Mineola, NY.

Ita, J. & King, S.D., 1994. Sensitivity of convection with an endothermic phase-change to the form of governing equations, initial conditions, boundary conditions, and equation of state, *J. geophys. Res.,* **99**(B8), 15 919–15 938.

Jarvis, G.T. & McKenzie, D.P., 1980. Convection in a compressible fluid with infinite Prandtl number, *J. Fluid Mech.,* **96,** 515–583.

Mihaljan, J.M., 1962. A rigorous exposition of the Boussinesq approximations applicable to a thin layer of fluid, *Astrophys. J.,* **136,** 1126–1133.

Moresi, V.N. & Solomatov, V.S., 1995. Numerical investigation of 2D convection with extremely large viscosity variations, *Phys. Fluids,* **7**(9), 2154–2162.

Schubert, G., Turcotte, D.L. & Olson, P., 2001. *Mantle Convection in the Earth and Planets,* 940 pp., Cambridge Univ. Press, New York.

Spiegel, E.A. & Veronis, G., 1960. On the Boussinesq approximation for a compressible fluid, *Astrophys. J.,* **131,** 442–447.

Tan, E. & Gurnis, M., 2005. Metastable superplumes and mantle compressibility, *Geophys. Res. Lett.,* **32,** L20307, doi:10.1029/2005GL024190.

Tan, E. & Gurnis, M., 2007. Compressible thermochemical convection and application to lower mantle structures, *J. geophys. Res.,* **112,** B06304, doi:10.1029/2006JB004505.

Turcotte, D.L., Hsui, A.T., Torrance, K.E. & Schubert, G., 1974. Influence of viscous dissipation on Benard convetion, *J. Fluid Mech.,* **64,** 369–374.

Zhang, S. & Yuen, D.A., 1996a. Various influences on plumes and dynamics in time-dependent, compressible mantle convection in 3-D spherical shell, *Phys. Earth planet. Inter.,* **94,** 241–267.

Zhang, S. & Yuen, D.A., 1996b. Intense local toroidal motion generated by variable viscosity compressible convection in 3-D spherical-shell, *Geophys. Res. Lett.,* **23**(22), 3135–3138.

Zhong, S., 2006. Constraints on thermochemical convection of the mantle from plume heat flux, plume excess temperature, and upper mantle temperature, *J. geophys. Res.,* **111,** B04409, doi:10.1029/2005JB003972.

Zhong, S. & Zuber, M.T., 2000. Long-wavelength topographic relaxation for self-gravitating planets and implications for the time-dependent compensation of surface topography, *J. geophys. Res.,* **105,** 4153–4164.

APPENDIX A: A MODIFIED UZAWA ALGORITHM FOR SOLVING THE COMPRESSIBLE STOKES FLOW PROBLEM

The momentum and mass equations for compressible Stokes flow problem are:

$$\tau_{ij,j} - p_{,j}\delta_{ij} = -[\rho_r Ra(T - T_r) - p\gamma]\delta_{i3}, \tag{A1}$$

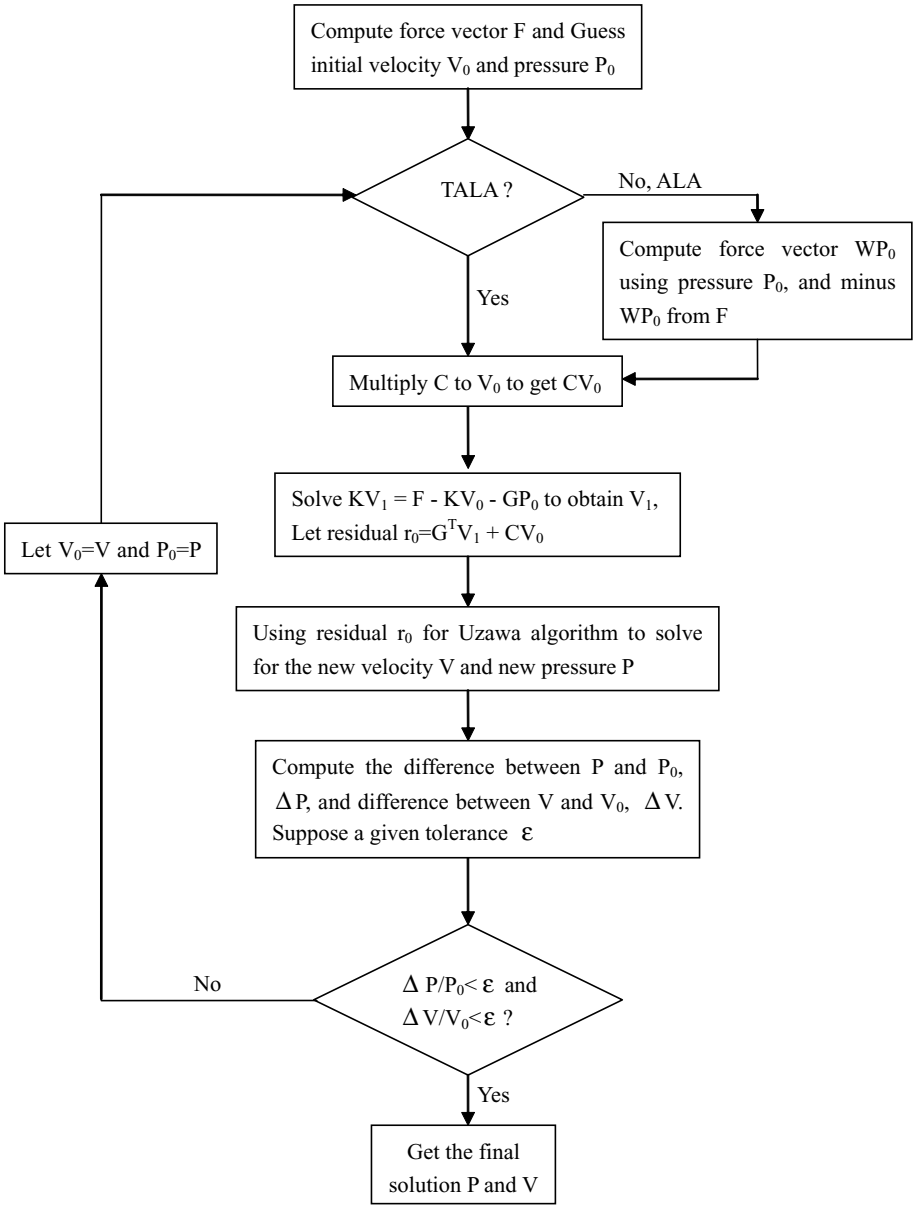

Figure A1. The flow chart of the modified Uzawa algorithm.

$$u_{i,i} + \frac{(\rho_r)_{,3}}{\rho_r} u_3 = 0. \tag{A2}$$

Following Hughes (2000), the corresponding matrix equation in finite element formulation is:

$$\begin{bmatrix} K & G+W \\ G^T + C & 0 \end{bmatrix} \begin{bmatrix} V \\ P \end{bmatrix} = \begin{bmatrix} F \\ 0 \end{bmatrix}, \tag{A3}$$

where V, P, K, G, G^T and F are the velocity vector, pressure vector, stiffness matrix, discrete gradient operator, discrete divergence operator and force vector, respectively. In contrast with the incompressible Stokes flow problem, we now have two additional terms: CV from the second term in eq. (A2) and WP from the buoyancy force associated with the dynamic pressure. Note that for TALA, vector WP is ignored.

In order to solve eq. (A3) with these additional terms, we modify the Uzawa algorithm. Fig. A1 shows the flow chart for the modified Uzawa algorithm. The key to our algorithm is to move the additional terms associated with compressibility to the right-hand side as part of the force term and to use an iterative method for a final stable solution. This is different from the bi-conjugate gradient method as employed recently in Tan & Gurnis (2007). The positive definite nature of the stiffness matrix **K** is preserved and the algorithm converges rapidly and appears to be stable. Our tests also show that our modified Uzawa algorithm does not add significant computational cost. Typically, after the first tens of time steps, it takes nearly the same computation time per time step for the compressible convection as for incompressible

convection calculations. Our modified Uzawa algorithm for compressible mantle convection is sufficiently general and is already extended to 3-D Cartesian and spherical models in codes CitcomCU and CitcomS.

APPENDIX B: ANALYTIC SOLUTION FOR 2-D COMPRESSIBLE STOKES FLOW PROBLEM

The 2-D compressible Stokes flow problem under ALA formulation can be described by the following equations:

$$\frac{\partial u}{\partial x}+\frac{\partial v}{\partial z}-v\gamma=0, \tag{B1}$$

$$\frac{\partial \sigma_{zz}}{\partial x}+\frac{\partial \tau_{xz}}{\partial z}+4\eta\frac{\partial^2 u}{\partial x^2}-2\eta\gamma\frac{\partial v}{\partial x}=0, \tag{B2}$$

$$\frac{\partial \tau_{xz}}{\partial x}+\frac{\partial \sigma_{zz}}{\partial z}+RaT\exp[(1-z)\gamma]-p\gamma=0, \tag{B3}$$

where u and v are velocity components in x and z directions; σ_{ij} is the stress tensor; τ_{ij} is the deviatoric stress tensor; the dynamic pressure p can be expressed as

$$p=\frac{4\eta}{3}\frac{\partial v}{\partial z}-\frac{2\eta}{3}\frac{\partial u}{\partial x}-\sigma_{zz}. \tag{B4}$$

Also note that

$$\tau_{xz}=\eta\left(\frac{\partial u}{\partial z}+\frac{\partial v}{\partial x}\right). \tag{B5}$$

We use trigonometric functions with wave number k to express these variables (Hager & O'Connell 1979).

$$u(x,z)=U(z)\sin(kx), \tag{B6}$$

$$v(x,z)=V(z)\cos(kx), \tag{B7}$$

$$\tau_{xz}(x,z)=Y_{xz}(z)\sin(kx), \tag{B8}$$

$$\sigma_{zz}(x,z)=S_{zz}(z)\cos(kx), \tag{B9}$$

$$T(x,z)=T_0(z)\cos(kx), \tag{B10}$$

where $U(z)$, $V(z)$, $Y_{xz}(z)$, $S_{zz}(z)$ and $T_0(z)$ are functions which only depend upon z. Substituting these variables into eqs (B1), (B2), (B3) and (B5), we obtain:

$$\frac{\mathrm{d}U}{\mathrm{d}z}=kV+\frac{1}{\eta}Y_{xz}, \tag{B11}$$

$$\frac{\mathrm{d}V}{\mathrm{d}z}=-kU+\gamma V, \tag{B12}$$

$$\frac{\mathrm{d}S_{zz}}{\mathrm{d}z}=-2\eta k\gamma U+\frac{4\eta}{3}\gamma^2 V-\gamma S_{zz}-kY_{xz}-Ra\Theta, \tag{B13}$$

$$\frac{\mathrm{d}Y_{xz}}{\mathrm{d}z}=4\eta k^2 U-2\eta k\gamma V+kS_{zz}, \tag{B14}$$

where $\Theta=T_0(z)\exp[(1-z)\gamma]$.

We can also write eqs (B11), (B12), (B13) and (B14) in matrix form as following:

$$\frac{\mathrm{d}}{\mathrm{d}z}\begin{bmatrix}V\\U\\S_{zz}/(2k)\\Y_{xz}/(2k)\end{bmatrix}=\begin{pmatrix}\gamma & -k & 0 & 0\\ k & 0 & 0 & \frac{2k}{\eta}\\ \frac{2\eta}{3k}\gamma^2 & \eta\gamma^2 & -\gamma & -k\\ -\eta\gamma & 2k\eta & k & 0\end{pmatrix}\begin{bmatrix}V\\U\\S_{zz}/(2k)\\Y_{xz}/(2k)\end{bmatrix}+\begin{pmatrix}0\\0\\-\frac{Ra\Theta}{2k}\\0\end{pmatrix}, \tag{B15}$$

Or

$$\frac{\mathrm{d}\chi}{\mathrm{d}z}=A\chi+\mathbf{b}, \tag{B16}$$

where $\chi=[V,U,S_{zz}/(2k),Y_{xz}/(2k)]^T$, $\mathbf{b}=\left(0,0,-\frac{Ra\Theta}{2k},0\right)^T$, and

$$A=\begin{pmatrix}\gamma & -k & 0 & 0\\ k & 0 & 0 & \frac{2k}{\eta}\\ \frac{2\eta}{3k}\gamma^2 & \eta\gamma^2 & -\gamma & -k\\ -\eta\gamma & 2k\eta & k & 0\end{pmatrix}. \tag{B17}$$

The solution of eq. (B16) can be expressed as:

$$\chi(z) = \exp[A(z - z_0)]\chi_0 + \int_{z_0}^{z} \exp[A(z-\xi)]\mathbf{b}(\xi)\mathrm{d}\xi$$
$$= P_A(z, z_0)\chi_0 + \int_{z_0}^{z} P_A(z, \xi)\mathbf{b}(\xi)\mathrm{d}\xi, \tag{B18}$$

where $\boldsymbol{\chi_0}$ is the starting vector at $z = z_0$, and $P_A(z, z_0)$ is the propagator matrix. For isoviscous cases with free-slip boundary conditions, $\eta = 1$, and V and Y_{xz} are both zeros at the top and bottom boundaries. Given Θ, Ra, k and γ, the horizontal velocity U and vertical stress S_{zz} at the top and bottom boundaries can be solved. We use $Ra = 1.0$ and $k = \pi$ in our models. $T_0(z)$ in Θ is given as a delta function in z direction at the middle depth of the system [i.e. $T_0(z) = \delta(z - 0.5)$].

For TALA, the analysis is the same except that the effect of dynamic pressure on the buoyancy term is ignored. The eq. (B3) therefore, becomes

$$\frac{\partial \tau_{xz}}{\partial x} + \frac{\partial \sigma_{zz}}{\partial z} + RaT\exp[(1 - z)\gamma] = 0 \tag{B19}$$

Consequently, the matrix equation becomes

$$\frac{\mathrm{d}}{\mathrm{d}z}\begin{bmatrix} V \\ U \\ S_{zz}/(2k) \\ Y_{xz}/(2k) \end{bmatrix} = \begin{pmatrix} \gamma & -k & 0 & 0 \\ k & 0 & 0 & \frac{2k}{\eta} \\ 0 & 0 & 0 & -k \\ -\eta\gamma & 2k\eta & k & 0 \end{pmatrix}\begin{bmatrix} V \\ U \\ S_{zz}/(2k) \\ Y_{xz}/(2k) \end{bmatrix} + \begin{pmatrix} 0 \\ 0 \\ -\frac{Ra\Theta}{2k} \\ 0 \end{pmatrix}. \tag{B20}$$

It should be pointed out that similar analyses were given by Tan & Gurnis (2007) and also in an unpublished note by Ita and Zhong.